SimBuild
2024

Eleventh National Conference of IBPSA-USA
Denver, Colorado
May 21 – 23, 2024

Early Design Thermal Comfort Modeling in Transient Conditions for Warming Hot Climates

Amber Jiayu Su[1], Christina Xingyizhen Brown[1], Remy Mermelstein[1], and Carlos Cerezo Davila[1]

[1]Kohn Pedersen Fox, New York, NY

Abstract

Short-term thermal history may have a substantial impact on how a person feels when traversing through urban spaces, especially in the context of global warming, as increasing temperatures and heat wave frequency will limit the quality and safety of their experience. While dynamic thermal comfort models such as Dynamic Thermal Sensation (DTS) are available, most analysis methodologies currently applied in urban design rely on steady-state models and tend to overlook the thermal history of occupants. This paper implements a DTS-based thermal comfort analysis workflow to predict the evolving thermal sensations of occupants along a path. The workflow is then applied in the analysis of a design project in Southeast Asia, to assess its effectiveness in evaluating design scenarios in comparison with a steady-state Universal Thermal Climate Index (UTCI) model.

Introduction

The issue of thermal comfort in urban and building space design has long been a focus of building performance simulation. However, it has gained even greater concern in the context of global warming and growing climate extremes. With the growing threat of extreme heat in urban areas and the resulting health concerns, it is important for designers to gain a deeper understanding of how occupants feel when traversing around the space to produce corresponding design solutions that ensure occupants' comfort and good experience. Most developed studies and modeling workflows applied in urban and building design tend to rely on metrics and comfort models that assume steady-state conditions, such as the Universal Thermal Climate Index (UTCI) (Jendritzky, et. al); however, in outdoor settings, human behavior and micro-climate are often dynamic and changing, and a thermoregulatory steady state requires at least 30 minutes to be achieved (Höppe 2002). In the built environment, people move through diverse thermal conditions, where an individual's perception depends highly on their past thermal experiences (Krüger et al., 2017). Disregarding this thermal history when evaluating thermal comfort may cause large inaccuracies, particularly for transitional spaces with considerable temperature differences, which not only results in discomfort but may also adversely influence human health (Lin et al., 2012). To design resilient urban spaces that stay vibrant in coming decades, it is critical to understand thermal comfort in unsteady and ambient environments, particularly in hot climates where the contrast between outdoor and indoor conditioned spaces will only increase with future temperature rise.

Published studies based on experimental data and thermal sensation surveys have shown that the temperature change rate of thermoreceptors is the driving factor for transient thermal comfort (Fiala et al., 2003; Zhang et al., 2010). Notably, when examining transexhibits conditions with noticeable differences, conventional physiological parameters like mean skin temperature, which typically exhibit a linear association with thermal sensation under stable conditions, show poor correlation in dynamic contexts (Du et al., 2014, Jia et al., 2023). The thermal sensation of individuals would change before these parameters adapt to the changing environment. Conversely, physiological parameters responsive to immediate environmental changes, such as skin temperature change rate, demonstrate more robust correlations with thermal sensation (Liu et al., 2014, Jia et al., 2023). Therefore, a thermoregulation model is necessary to compute these physiological parameters as inputs for a dynamic thermal sensation evaluation. In this context, two-node human thermoregulation models that divide the body into two concentric parts, have been developed to scrutinize the dynamic adaptation of both skin and core body temperatures in these transient conditions (Gagge et al. 1971, Höppe 1993). Furthermore, in recent years, more intricate multi-node and multi-element models have emerged, which dissect the human body into various segments to account for localized heat transfer and influence (Al-Othmani et al. 2008, Zhang et al., 2010). While several models have been developed and validated within controlled laboratory settings and real-world environments, the practical application of dynamic thermal comfort modeling in addressing real design challenges remains notably limited. This study aims to bridge this gap by implementing and integrating a two-node thermoregulatory bioheat model with Fiala's Dynamic Thermal Sensation (DTS) model within a design-focused modeling environment. Although multi-node models exhibited heightened reliability and accuracy, we chose to implement the simpler two-node model for its computational efficiency and practicality to apply in the early design phase when limited personal and environmental parameters are available. Despite its simplicity, prior research on the application of the two-node model indicates its accuracy through preliminary validation against other experimental and analytical data (Katavoutas et al, 2015, Zolfaghari & Maerefat, 2010). The integrated framework is implemented within the Rhinoceros 3D software (Mcneel. 2020) that allows designers to gain a more comprehensive understanding of the sensory experience of occupants in a transient condition from an early design stage. Additionally, to enhance the consideration of the local micro-climate's influence, computational fluid dynamics (CFD) is employed to simulate wind, enabling a more precise assessment of the impact of building geometries on wind speed. Table 1 provides a comparison of features between our proposed workflow and other commonly used thermal comfort analysis tools.

Table 1 Comparison between Proposed Workflow and other Tools

	Rhino-Integrated Workflow	CFD Integration	Static Comfort	Dynamic Comfort
Proposed Workflow	●	●	●	●
Eddy3d	●	●	●	
Envi-Met		●	●	available in beta version
Solweig	●		●	
Rayman	●		●	

The proposed workflow is subsequently applied to a specific design scenario - a mixed-use project in Southeast Asia - to better understand its impact on design decision making. We conducted a comparative analysis between the thermal comfort results rendered by both a best-practice steady-state UTCI-based modeling workflow and the proposed dynamic modeling workflow to understand the difference of thermal sensation relative to the same occupant path. This comparison extends to both current (2023) and future (2080) projected climate conditions, highlighting the capacity of dynamic thermal modeling to uncover design parameters and opportunities that the UTCI-based model could not capture or assess.

Background

To implement this workflow, we chose the two-node thermoregulatory bioheat model developed by Peter Höppe to obtain the physiological parameters and Dynamic Thermal Sensation developed by Fiala to quantify thermal sensation in transient context. The formulation of each step implemented in the modeling workflow is detailed below:

Two-node Thermoregulatory Bioheat Model

The Instationary Munich Energy Balance Model (IMEM) is a two-node bioheat model (Höppe 1993), that divides the human body into two concentric cylinders – the outer shell that represents the skin layer, and the inner shell that represents the core. IMEM takes into consideration the thermoregulatory reactions of human bodies in different thermal conditions, including sweating, shivering, convection, metabolic work, and peripheral vasomotoric processes. IMEM consists of three fundamental equations.

The overall heat storage S can be calculated through the sum of heat losses and gains:

$$H + C + R + E_D + E_{Res} + E_{Re1} + E_{sw} = S \quad (1)$$

where H is the internal heat gain where (shivering and metabolic heat are included), C is the convective heat flux, R is the radiative heat flux, E_D is the heat flux through skin vapor diffusion, E_{Res} is the heat flux through the heating of the inspired air, R_{Rel} is the heat flux through the humidification of the inspired air and E_{sw} is the heat loss through sweating.

The second function is that:

$$F_{sc} = \frac{1}{l_{cl}} (Tsk - Tcl) \quad (2)$$

where F_{sc} is the heat flow from the skin surface to the cloth surface, l_{cl} is the heat transfer resistance of the clothing, T_{sk} is the skin temperature, and T_{cl} is the clothing surface temperature. Assuming that clothing layer has no heat capacity, F_{sc} should be equal to the sum of the convective and the radiative heat flux. If the skin temperature is known, the clothing surface temperature could be calculated; and therefore, all the heat fluxes described above, and the overall heat storage S could be calculated subsequently.

The third function describes the heat flux from the core to the skin:

$$F_{cs} = v_b \times \rho_b \times c_b \times (T_c - T_{sk}) \quad (3)$$

in which F_{cs} is the heat flow from the core to the skin, v_b is the blood flow from the core to the skin, ρ_b is the blood density, c_b is the specific heat and T_c is the core temperature.

With the third function, the core heat storage S_c and skin heat storage S_s could be calculated separately, were

$$S_c = H + E_{Res} + E_{Rel} - F_{cs} \quad (4)$$

$$S_s = F_{cs} + C + R + E_D + E_{sw} \quad (5)$$

The last unknown piece for the skin and the core temperature change rates calculation is the proportion of the skin and the core. Höppe uses the following equation to calculate the mass distribution alpha of body shell to the whole body:

$$alpha = 0.44 + \frac{0.35}{(v_b - 0.1386)} \quad (6)$$

With all these pieces, the skin and the core temperature change rate could then be calculated by:

$$S_s = M \times alpha \times c_k \times \frac{dT_s}{dt} \quad (7)$$

$$S_c = M \times (1 - alpha) \times c_k \times \frac{dT_c}{dt} \quad (8)$$

where M is the body weight and c_k is the specific heat of body.

Dynamic Thermal Sensation (DTS)Model

Fiala's dynamic thermal sensation model is developed based on a large number of experimental thermal sensation votes and related body parameters; through correlation analysis, Fiala had identified that core temperature, skin temperature and skin temperature change rate are the three affecting parameters. Through regression analysis, a function composed of three parts had been developed to predict whole-body thermal sensation on the ASHRAE seven-point scale. The complete calculation is as follow:

$$DTS = 3 \times \tanh(f_{sk} + \phi + \psi) \quad (9)$$

where:

$$f_{sk} = 1.08 \times \triangle T_{sk,m} \left(for \triangle T_{sk,m} > 0\right)$$
$$f_{sk} = 0.30 \times \triangle T_{sk,m} \left(for \triangle T_{sk,m} < 0\right) \quad (10)$$

$\triangle T_{sk,m}$ is the deviation of mean skin temperature to the neutral skin temperature point, which equals to $T_{mean\,skin} - 34.4$

$$\phi = 7.94 \times \exp\left(-0.902 / \left(\Delta T_{hy} + 0.4\right) + 7.612 / \left(\Delta T_{sk,m} - 4\right)\right)$$
$$\phi = 0 \; when \; \Delta T_{hy} + 0.4 \leq 0 \; or \; \Delta T_{sk,m} - 4 \geq 0 \quad (11)$$

ΔT_{hy} Is the deviation of core temperature from the core neutral point, which equals to $T_{hypothalamic} - 37.0$

$$\psi = (\tau_- + \tau_+) / (1 + \phi)$$
$$\tau_- = 0.11 \times dT_{sk,m}/d_t \left(when\; dT_{sk,m}/d_t < 0\right)$$
$$\tau_+ = 1.91 \times \left(dT_{sk,m}/d_t\right)_{max} \times \exp\left(-0.681 \times \Delta t\right)\left(when\; dT_{sk,m}/d_t > 0\right) \quad (12)$$

where Δt is the time between the current time and the time when the highest skin change rate happen.

f_{sk} and ϕ deal with the static part of thermal sensation accounting for the effects associated with both the skin's and core's temperature deviations from their neutral points, while ψ accounts for the dynamic response to the immediate change that are observed in transient conditions using skin temperature change rate.

Methodology

The process of implementing the proposed modeling workflow and applying it to the case study project required the development of a custom calculation component within Rhinoceros 3D and its scripting environment Grasshopper. The following sections detail how each step of the process was adapted to the modeling environment and data sources used, in order to map dynamic and steady thermal comfort conditions along a 3D path (Figure 1).

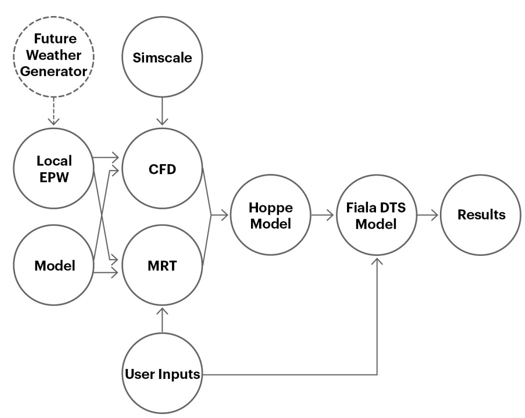

Figure 1: Proposed modeling workflow

Model Geometry Processing

To understand dynamic thermal comfort, a specific path has to be defined that represents how an individual traverses this space. The workflow relies on an early design 3D urban model (including building massing, ground, and shading structures) and an analysis pedestrian path defined as a polyline or curve. The user-defined path in Rhino is automatically divided into multiple discrete points, representative of a timestep so that related environmental and personal data of each point can be collected. The following data processing and calculation of Dynamic and UTCI-based comfort metrics are performed at each point.

Data Extraction and Simulation

Once geometry has been processed, the calculation entails the application of Höppe's two-node thermoregulatory model, which facilitates the computation of core temperature, skin temperature, and skin temperature change rate, and Fiala's DTS model to quantify thermal sensation based on the obtained physiological parameters. Through this calculation process, the thermal comfort assessment is conducted for each discrete point along the traversed path. This process requires the estimation of several environmental and personal parameters based on local microclimate conditions, building form, and assumed pedestrian characteristics.

Basic local climate parameters for the time period of interest, including air temperature, dew-point temperature, and air pressure, are directly extracted from a local EPW weather file in TMYx (1956-2021) format. The remaining environmental data include the mean radiant temperature (MRT) and wind speed, which are derived through solar radiation and CFD wind simulations at each point, capturing the impacts of both the architectural design and its surrounding context. MRT data is computed through a custom script, combining the sky view ratio, solar altitude, and the diffuse and direct radiation obtained from the calculated sky matrix. using Ladybug (Ladybug Tools LLC, 2021). Wind simulation data is obtained from a CFD model, working directly of the Rhino modeling environment through a custom API for the cloud-hosted simulation service Simscale (Heiny et al. 2012). The developed workflow automates the process of sending the analysis geometry for simulation and extracting the monthly prevailing wind direction and average wind speed from the weather file. Later, the custom script retrieves wind speed results from the simulation platform, and scale wind speeds to each modeled point by a ratio calculated according to their height in relation to weather station data and terrain roughness of the location, both user inputs. The last segment of the dataset pertains to occupant parameters. Recognizing that factors such as age, gender, and body parameters impact an individual's response to their external surroundings, thus these parameters have been configured as user-defined inputs to facilitate modeling for different occupant groups. For example, clothing level (CLO) and metabolic rate (MET) are two factors that directly affect the thermoregulatory response of an individual, and thus can be adjusted given the analysis needs.

Dynamic Thermal Sensation Calculation

Based on the simulated and extracted data in previous steps for each analysis point within the analysis path, the proposed workflow automates a 2-step calculation of a dynamic thermal comfort metric: First, a two-node thermoregulatory model is calculated taking into consideration heat flows around the human body. Second, Fiala's DTS calculation is performed based on step 1 results, creating a comfort index based on ASHRAE's seven-point scale (ASHRAE, 1992).

In the proposed workflow implementation, the initial core and skin temperatures may be determined by means of the two-node model, presuming that steady state has been reached at the beginning of the analysis, or they may be specified by the user. With the initial body temperatures and personal and environmental parameters as input for each point of interest, the heat storage (S) could be calculated at each point according to the formula above. Simultaneously, in conjunction with the heat transfer equation delineating the thermal exchange dynamics between the core and the skin, it becomes possible to independently compute temperature change rates for both the skin and the core. These rates are integrated over discrete time intervals, based on the point divisions in the analysis path, culminating in the derivation of initial temperatures at each point. This iterative computation process establishes the requisite input variables, namely skin temperature change rate, skin temperature, and core temperature, for the DTS model at each location. Subsequently, the DTS comfort could be assessed at each point along the path.

Case Study

To evaluate the application and impact of the transient thermal workflow developed, we conducted a comparative analysis between UTCI and transient thermal comfort for a Southeast Asia mixed-use development based on a real design project by the authors. The case study was developed to analyze thermal comfort in key paths and evaluate how the two metrics might affect design decisions differently. The project is located near the equator; thus, it experiences a tropical climate with fairly uniform temperatures and high humidity all year round. The project consists of mainly two large towers of varying heights with a unified podium design that provides many outdoor program spaces as well as open-air circulation to the podium rooftop. The open-air circulation is design-oriented relative to the local predominant wind directions with the intent of enhancing comfortable breezes through space. The podium roof is also fully accessible, with the intent of providing occupants with an enjoyable yet comfortable outdoor experience traversing through the project. Three paths were developed to best represent the extremes in site usage – first path (A) aimed to take the most direct and solar exposed path without the design context, second path (B) walking around the perimeter of the site for the most solar exposure with context included, and the third path (C) aimed to move through the various thermal transition spaces (Figure 2). All paths have a length of 300 m, equivalent to a walk of approximately 4.5 minutes, assuming a typical walking speed of 1.1 m/s.

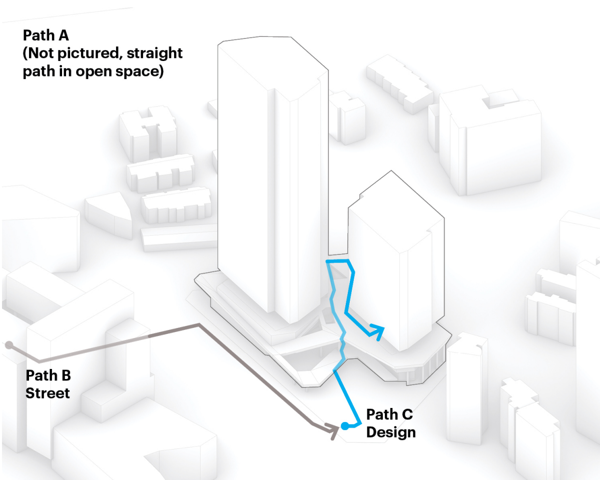

Figure 2: Case study massing model and analysis paths

For better comparison, UTCI results for the steady state case are converted into an equivalent thermal sensation metric based on the work of Zare et. Al (Zare et al, 2018). For the purposes of the case study, we set the initial skin and core temperatures to 34.4°C and 36.9°C respectively, and metabolic rate (MET) as 2.3 in accordance with the foundational assumptions in the original UTCI calculation (Jendritzky et al, 2002). In consideration of the geographical context of the project location, we used parameters corresponding to the average office worker's characteristics (age, weight, and height) and assumed a climate-appropriate clothing insulation value (CLO) of 0.57.

For the purposes of the study, two EPW weather files were used to represent current and future conditions: a TMYx (1956-2021) file encompassing the climate averages as we know it; and a morphed version of the same weather file to the year 2080. Morphing was done using a future weather generator for building performance research developed by Rodrigues et. al (Rodrigues et al. 2023). The tool allows for morphing using EC-Earth3 and CMIP6 model scenarios, which served as the basis for the 6th IPCC Assessment Report, published in 2022 (Rodrigues et al, 2023). The 20-year mean difference between the model performance against reanalysis from the ERA40 dataset, long considered the gold standard, was 1.2% for air temperature, 0.8% for net thermal radiation, and 0.7% for specific humidity. CMIP6 on the other hand has a resolution roughly 2/3 that of EC-Earth3 and 5 to 10% less accuracy compared to the same ERA40; therefore, EC-Earth6 was chosen for our case study. The morphing mathematically transforms using a delta procedure between the current EPW and future weather scenarios to create a new EPW file which is then input into the case study. In general, temperature estimates in the EPW file increase by 1 to 4°C by 2080, humidity increases by 5% to 10%, and wind speeds decrease slightly or remain the same, as does radiation. In both cases, the analyses were conducted on October 11th at noon in alignment with the design project local regulation's default assumptions for all UTCI calculations.

Result

The developed workflow allowed for successfully model thermal comfort using both the proposed DTS-based dynamic index, and a UTCI steady state index. The results detailed below report UTCI and DTS metrics compared along the three paths chosen (A, B, and C), for both current and future climate conditions. For both metrics, the index scale used, based on ASHRAE's 7-point thermal sensation scale, ranges from -3 (Cold) to +3 (Hot) with 0 representing a neutral thermal condition, and comfort defined between -1 and 1.

In Figure 3, 'A - Open Field' displays the thermal comfort of a person walking for 300 m in an open area absent of any obstructions. According to the UTCI based index, upon departing from a state of initial comfort, the individual promptly transitions to a state of extreme discomfort, which persists throughout the entire path without any discernible variation. Conversely, the DTS index for 'A - Open Field' shows that starting from the same level of comfort, the individual first has a sharp increase of discomfort before shifting towards a prolonged slow increase of discomfort as the distance continues. Assuming at the end of this path, the user immediately enters a conditioned, comfortable space, the UTCI index plunges back into comfort, while it takes roughly 1.5 minutes for the DTS index to reach comfort again.

In the second path where the user walks around the periphery of the site (noted in Figure 3 as ‘B - Street’), the UTCI index follows the exact same trend as in the first path. However, the DTS index instead demonstrates variations in comfort due to the surrounding design contextual buildings providing shade and moments of comfort throughout the path. This impact results in an overall lower heat discomfort, which also results in a shorter amount of time needed to reach comfort upon the end of the 300m path.

In the third path (noted in Figure 3 as ‘C - Design’), the two indices exhibit notable distinctions, especially in the case of thermal step change. Starting from a state of comfort, both the static and dynamic indices indicate a rapid increase in discomfort as the user traverses an area fully exposed to radiation. Upon entering the shaded region beneath the podium roof canopy, the static index registers a modest decrease in discomfort, whereas the dynamic index demonstrates a stronger effect of shading in alleviating discomfort, which may be attributed to the dynamic comfort index's incorporation of skin temperature change rate, reflecting the body's response to thermal step change. Subsequently, as the user progresses into the interior space with lower air temperatures, the dynamic index portrays a sudden transition from warmth to slight cool before ultimately reaching a state of comfort. In contrast, the static index implies that the user promptly attains a state of comfort upon entering the indoor environment.

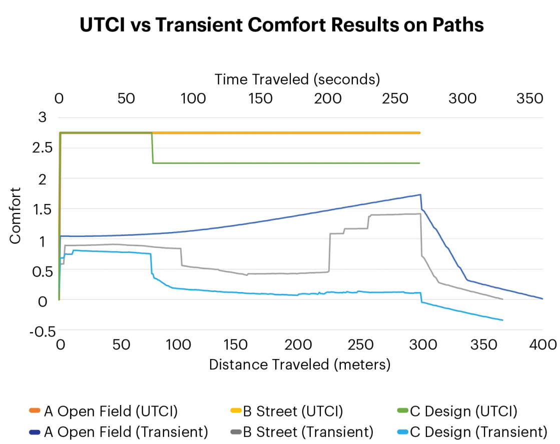

Figure 3 UTCI vs Transient Comfort Results for 3 Paths

The results for the same 3 paths with 2080 projected weather data yield are shown in figure 4. Though the UTCI index only showed a small increase in discomfort, the DTS index changed more drastically. Path A increased in heat discomfort but retained the same trend. The increase in temperatures however, removed from path B the benefits of context shading, matching path A in levels of discomfort. Lastly, path C also increased in heat discomfort with a more noticeable jump when the occupant would be first arriving on the podium roof. In all cases, the distance or time required for the occupant to reach comfort once in the conditioned interior increased, with 50-60 more meters required in paths A and B versus the more protected path C.

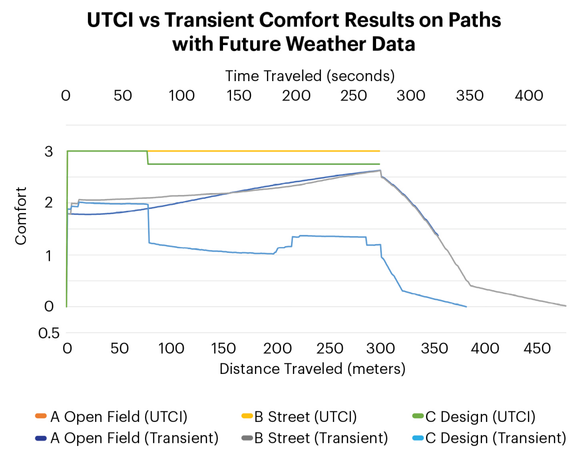

Figure 4 UTCI vs Transient Comfort Results for 3 Paths with Future Weather Data

To further understand how the two indexes perform, and compare the time required to achieve comfort indoor after walking outside, we simulated an additional scenario similar to path A (Open field condition) for a longer maximum distance of 2000 m. In many cases, including scenarios simulating a hypothetical warmer climate in 2080, it takes, on average, over 300 m for a pedestrian to reach a state of discomfort according to the dynamic index, whereas the static index already categorizes the user as experiencing discomfort from the moment they depart from a comfortable location, as shown in figures 5 and 6. Similarly, the UTCI based index assumes immediate comfort when walking indoors at the end of the path, regardless of the length of the walk outside, while the DTS index shows how the longer the walk the longer the thermal recovery. For example, a 15-minute walk in current climate conditions would require approximately 2 minutes indoors to recover comfort, while by 2080 it would require close to 6 minutes.

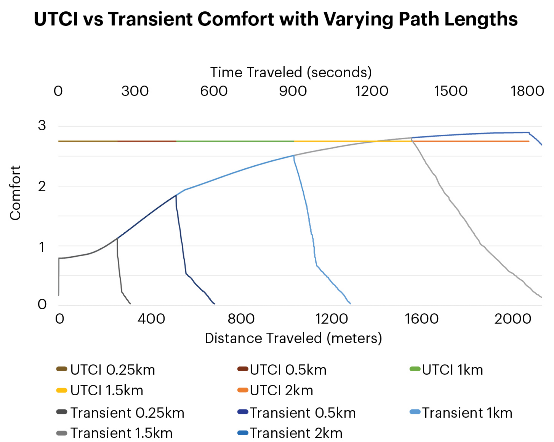

Figure 5 UTCI vs Transient Comfort with Varying Path Lengths

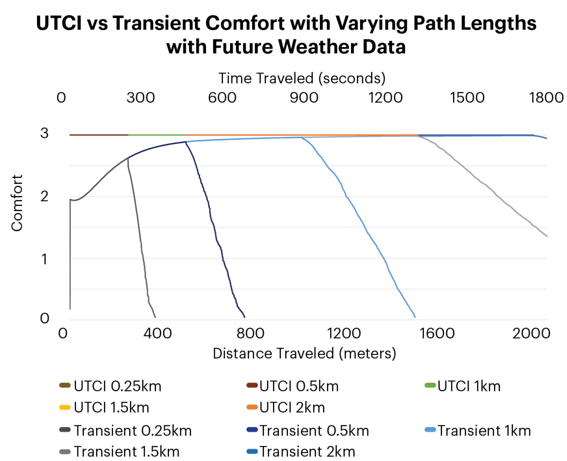

Figure 6 UTCI vs Transient Comfort with Varying Path Lengths with Future Weather Data

Discussion

This paper has shown how it is already possible to integrate complex dynamic thermal comfort models into architectural design modeling tools, such as Rhinoceros 3D, making them accessible to designers in the early stages of a project. Why is this important? Our findings indicate that the generally adopted outdoor thermal comfort metrics, like UTCI, cannot effectively discern the intricate effects of transient environmental factors, such as radiation, which are revealed by the dynamic index like DTS. By incorporating the rate of change in skin temperature, the dynamic index accounts for immediate environmental changes and their impact on the user's thermal comfort. This approach offers designers a more comprehensive understanding of how their designs influence the thermal comfort of individuals as they traverse through a given space, and as they transition from unconditioned to conditioned environments. The results of the case study illustrate the pitfalls of relying on a static outdoor comfort index such as the UTCI for designing for comfort in a hot and humid climate. As outlined in the previous section, three paths were chosen to highlight the potential different thermal experiences of a user along the site. Noticeable differences are present in all three paths between UTCI and the dynamic index. UTCI fails to account for the delay in the rate of change for comfort indexes and cannot illustrate how important gradual transitions become in climates where the difference between indoor and outdoor temperatures are drastic. This is not to say however, that UTCI indexes are not valuable in design, as both static and dynamic indexes render equivalent results after a user has been in a space for a certain amount of time in the 20-30 minutes range. UTCI and other static indexes seem appropriate for the design of seating areas for example in plazas or terraces, while dynamic indexes seem better suited for pedestrian experiences and indoor-outdoor transitions. Recognizing that the user inputs – such as clothing level and metabolic rate – can differ by program, regionality, and other project-specific factors, the authors intend to explore the impacts of input changes across regional differences through the application across a diverse range of projects and locales in a future study.

In contrast, the DTS dynamic comfort index reveals interesting design challenges that will become more relevant for designers as global warming accelerates. For example, it is entirely possible that a user in an outdoor setting that has been designed with high albedo materials, shade, and wind comfort can remain in relative comfort with little extra intervention even in a hot humid environment. A static index might suggest that one needs to over-design the same space to achieve the same level of comfort. This may lead designers to take a semi-conditioned, or non-conditioned space, such as the case study's podium open air circulation, and condition it, for fear of it being uncomfortable for the users. The integration of the DTS index in a design modeling tool enables designing such spaces as an interesting opportunity to allow for a new way of thinking spatially. A designer can guide an occupant through gradual thermal comfort transitions in anticipation of them entering a comfortably conditioned space at the end of their journey. This involves designing a buffer that accounts for the additional time the dynamic index says it will take to reach comfort from an uncomfortable place. This paper employs dynamic thermal comfort simulation within a design case just to showcase its practical application and implications during the design process. However, its effectiveness and accuracy need to be assessed through validation. The authors plan to pursue subsequent research that will entail performing experiments within existing buildings and comparing the empirical results with simulation outcomes to understand the model's accuracy.

While the selection of the two-node heat transfer model and the dynamic thermal sensation model is motivated by their simplicity and applicability during the early design stages, prior research indicates that the utilization of more intricate models, such as the multi-node heat balance model and dynamic thermal sensation models incorporating local skin temperature, yields greater precision and reveals finer nuances in thermal sensation assessment. However, these models require greater time demands and may pose potential challenges in acquiring or making assumptions regarding input data at the initial design phase. Consequently, it would also be advantageous to compare this workflow with other simulation models to understand the tradeoffs.

Additionally, the authors believe that the workflow proposed could be further enhanced by incorporating an automated route generator, facilitating the execution of dynamic thermal comfort simulations on a multitude of generated routes. By collectively examining the results obtained from various routes, one can gain insights into specific areas where a significant portion of the population might experience thermal discomfort while traversing through the specified locations. This comprehensive approach to dynamic thermal comfort analysis is instrumental in providing a holistic understanding of the transient thermal comfort across the building site.

Conclusion

Thermal history has a significant impact on the thermal comfort of occupants in transient settings. Conventional thermal analysis workflows, in such scenarios, may lead to an overestimation or underestimation of an occupant's thermal sensation. While UTCI evaluates the thermal comfort of an area comprehensively, for example in an urban scale assessment; in those cases where certain movement paths dominate, the conventional thermal comfort analysis may fail to predict the evolving sensations as users move through those paths, especially in places with thermal step changes. Our findings suggest that the dynamic index, as proposed in this study, offers a more meaningful and nuanced perspective for designers, particularly for transitional spaces. This model proves to be a valuable tool for predicting thermal comfort, even in the early design stages. Further studies are planned for validation against experimental data in built projects and the application of this workflow in different climates.

References

Al-Othmani M, Ghaddar N, Ghali K (2008) A multi-segmented human bioheat model for transient and asymmetric radiative environments. Int J Heat Mass Transfer 51:5522–5533

Du, X., Li, B., Liu, H., Yang, D., Yu, W., Liao, J., Huang, Z., & Xia, K. (2014). The response of human thermal sensation and its prediction to temperature step-change (cool-neutral-cool). PloS one, 9(8), e104320.

Fiala, D., Lomas, K., & Stohrer, M. (2003). First Principles Modeling of Thermal Sensation Responses in Steady-State and Transient Conditions. ASHRAE Transactions, 109, 179–186.

Gagge, A.P., Stolwijk, J. and Nishi, Y. 1971, An Effective Temperature Scale Based on a Simple Model of Human Physiological Regulatory Response. ASHRAE Transactions, 77, 247-262.

Heiny, D., Dolle, V., Probst, J., Fischer, A., & Dammer, A. (2012). SimScale. [computer software] https://www.simscale.com Höppe, P. R. (1993). Heat balance modelling. Experientia, 49(9), 741–746.

Höppe, P. R. (2002). Different Aspect Assess Indoor Outdoor Thermal Comfort., 34 (6), 661–665.

Jendritzky, G., Maarouf, A. R., Fiala, D., & Staiger, H. (2002). J5B.4 An Update on the Development of a Universal Thermal Climate Index.

Jia, X., Li, S., Zhu, Y., Ji, W., & Cao, B. (2023). Transient thermal comfort and physiological responses following a step change in activity status under summer indoor environments. Energy and Buildings, 285, 112918.

Katavoutas, G., Flocas, H. A., & Matzarakis, A. (2015). Dynamic modeling of human thermal comfort after the transition from an indoor to an outdoor hot environment. International Journal of Biometeorology, 59(2), 205–216.

Krüger, E. L., Tamura, C. A., Bröde, P., Schweiker, M., & Wagner, A. (2017). Short- and long-term acclimatization in outdoor spaces: Exposure time, seasonal and heatwave adaptation effects. Building and Environment, 116, 17–29.

Ladybug Tools LLC(2021) Ladybug Tools. (Version 1.4.0) [Computer software]. www.ladybug.tools.

Lin, S., Insaf, T. Z., Luo, M., & Hwang, S.-A. (2012). The effects of ambient temperature variation on respiratory hospitalizations in summer, New York

State. International Journal of Occupational and Environmental Health, 18(3), 188–197.

Liu, H., Liao, J., Yang, D., Du, X., Hu, P., Yang, Y., & Li, B. (2014). The response of human thermal perception and skin temperature to step-change transient thermal environments. Building and Environment, 73, 232-238.

McNeel, R. (2020). Rhino3D (Version 7.n) [Computer software]. https://www.rhino3d.com/

Rodrigues, E., Fernandes, M. S., Carvalho, D. (2023). Future weather generator for building performance research: An open-source morphing tool and an application. Building and Environment, 233, 110104.

Standard, A. S. H. R. A. E. (1992). Thermal environmental conditions for human occupancy. ANSI/ASHRAE, 55, 5.

Zare, S., Hasheminejad, N., Elahi Shirvan, H., Hemmatjo, R., Sarebanzadeh, K., & Ahmadi, S. (2018). Comparing Universal Thermal Climate Index (UTCI) with selected thermal indices/environmental parameters during 12 months of the year. Weather and Climate Extremes, 19, 49-57.

Zhang, H., Arens, E., Huizenga, C., & Han, T. (2010). Thermal sensation and comfort models for non-uniform and transient environments, part III: Whole-body sensation and comfort. 1st International Symposium on Sustainable Healthy Buildings, 45(2), 399–410.

Zolfaghari, A., & Maerefat, M. (2010). A new simplified thermoregulatory bioheat model for evaluating thermal response of the human body to transient environments. Building and Environment, 45(10), 2068-2076.